A Conservative, Scalable, Space-Time Blade Element Rotor Model for Multi-rotor Vehicles

Jonathan J. Chiew
Ph.D. Candidate,
Stanford University,
Stanford, CA

Michael J. Aftosmis
Senior Research Scientist,
NASA Ames Research Center,
Moffett Field, CA

August 1, 2017

Abstract

The development of a parallel blade-element rotor model and its implementation into an adaptive Cartesian method is described. The unsteady version of the rotor model applies a body force to all cells contained in the swept space-time volume at each timestep and special care is taken to maintain axisymmetry on the Cartesian grid. Mesh convergence of rotor thrust and torque is obtained with around 10000 cells in the disk for the steady model. Parallelization is accomplished using OpenMP and the rotor force computation is distributed across all available nodes. Simulations of an isolated XV-15 rotor in hover show good correlation with experimental data and predictions of multi-rotor thrust variation closely match previous high fidelity simulations. *The final paper will also include results from the unsteady rotor model and parallel scaling tests.*

1 Introduction

In recent years, the aerospace industry has seen dramatic growth in the small unmanned vehicle sector for both commercial and recreational purposes. A variety of multi-rotor concept vehicles have been proposed which take advantage of the benefits of electric propulsion to provide vertical take-off and landing (VTOL) capability using open rotors or ducted fans.

Early in the design cycle, particularly for smaller scale UAS (Unmanned Aircraft System) development, time-accurate Computational Fluid Dynamics (CFD) analysis is generally infeasible due to the long turn-around times, especially for designers with limited access to high-performance computing resources. Alternatively, a variety of tools with rapid turnaround times exist, but they are typically limited to low fidelity (linear) aerodynamics.

In this work we describe the development a medium-fidelity rotor aerodynamics model and begin to explore its suitability for aerodynamic design of multi-rotor aircraft.

2 Governing Equations and Numerical Method

The three dimensional Euler equations governing inviscid flow of a calorically perfect gas for a control volume Ω with closed boundary $\partial\Omega$ may be written as

$$\iiint_{\Omega} \frac{\partial \mathbf{U}}{\partial t} dV + \oint_{\partial\Omega} \mathbf{F} \cdot \hat{n}\, dS = \iiint_{\Omega} \mathbf{S}\, dV \tag{1}$$

where $\mathbf{U}$ is the vector of conserved variables,

$$\mathbf{U} = [\rho, \rho u, \rho v, \rho w, \rho E]^T \tag{2}$$

$\mathbf{F}$ is the flux density tensor,

$$\mathbf{F} = \begin{bmatrix} \rho u & \rho u^2 + p & \rho uv & \rho uw & u(\rho E + p) \\ \rho v & \rho uv & \rho v^2 + p & \rho vw & v(\rho E + p) \\ \rho w & \rho uw & \rho vw & \rho w^2 + p & w(\rho E + p) \end{bmatrix}^T \tag{3}$$

$\hat{n}$ is the outward facing unit normal vector, ρ is the fluid density, u, v, and w are the Cartesian velocity components, p is the fluid pressure, E is the total energy per unit mass, and S is an arbitrary body-force vector.

The rotor model is implemented in a widely used simulation framework which solves the governing equations (1) using a multilevel Cartesian mesh with embedded boundaries [1]. The mesh consists of regular Cartesian hexahedra everywhere, except for a layer of cut cells, which are cells clipped into arbitrarily shaped polyhedra by the body of interest. The spatial discretization uses a second-order, finite volume approach with a weak imposition of boundary conditions. Time-dependent flow solutions utilize dual-time stepping where a Runge-Kutta based multigrid smoother drives an implicit second-order, backward difference time integration scheme similar to [6].

3 Rotor Modeling

Typical high-fidelity rotor simulations with discrete blade geometry require tens of millions of mesh points per rotor and thousands of timesteps for accurate force predictions [2], [5], [13]. Although an isolated rotor in hover can be cast as a steady-state problem in a non-inertial reference frame, this simplification is not general enough for maneuvering flight or multi-rotor vehicles.

Actuator disk and blade element rotor models have seen widespread usage for modeling propellers and rotor-airframe interactions. In his review article, Le Chuiton [7] describes how these models can be implemented either as source terms, fluxes, or boundary conditions. In order to support multiple arbitrarily oriented rotors, the source term approach (which does not constrain the computational mesh to align with each rotor plane) is chosen in this work. Rather than embedding a polar rotor grid into the volume mesh as is typical [9], we implement the model using the existing Cartesian volume cells, as described in the following section.

In addition, the rotor model smoothly transitions between steady and time-accurate modes. It is similar to previous work on actuator surface [10], actuator line [12], or actuator blade [9] models, but the chordwise distribution is chosen to include the wedge of the rotor disk swept by each blade during that timestep.

3.1 Rotor Cells

The rotor model's body force terms are only applied to the Cartesian hexahedra that intersect the rotor disks. These "rotor hexes" are identified once in parallel preprocessing step. Note that the unsteady rotor model uses static meshes with a rotating source term, so this search is only performed once for time-dependent simulations as well. First, the minimum Cartesian bounding box that contains each rotor is computed from the rotor hub center, radius, and shaft axis user inputs. Next, the intersection of the rotor plane and each cell within this bounding box is computed. The general intersection of a Cartesian hexahedron and a plane is a polygon with 3-6 vertices (away from degeneracies). The polygon vertices are then linearly trimmed based on non-dimensional radius to remove all points which have $r/R > 1$ or $r/R < r_0$ (the root cutout). Finally, the area of the polygon, which is needed to scale the rotor source terms, is computed via triangulation.

3.2 Rotor Source Terms

Since we are using a compressible flow solver, both the momentum and energy equations contain source terms arising from the body force. Mass is conserved for conventional rotors not employing tip jets, Coanda jets, etc. The rotor source term, $\mathcal{S}$ in (1), is defined as

$$\mathcal{S} = [0, \mathbf{F_r} \cdot \hat{e}_x, \mathbf{F_r} \cdot \hat{e}_y, \mathbf{F_r} \cdot \hat{e}_z, \mathbf{F_r} \cdot \mathbf{u}]^T \tag{4}$$

where $\mathbf{F_r}$ is the local rotor force computed from blade element theory, $\mathbf{u}$ is the local velocity vector, and $\hat{e_i}$ is the unit vector in the i coordinate direction. The forces computed from blade element theory [8] are scaled by the time the blade spends in each cell as in [9]. This scaling factor f_{sc} is defined as

$$f_{sc} = \frac{N_b \, \Delta\psi}{2\pi} = \frac{N_b \, \Delta\psi}{2\pi} \frac{r\Delta r}{r\Delta r} = \frac{N_b A_c}{A_a} \tag{5}$$

where A_c is the area of the cell as computed above, A_a is the area of the annulus, $\Delta\psi$ is the azimuthal span of the cell, r is the cell's radial position, and Δr is the cell's radial span. For Cartesian cells, special care is required to (approximately) maintain azimuthal symmetry: Δr is defined as the radius of a circle with area A_c in the computation of A_a. Figure 1 shows how this retains the azimuthal symmetry of the distribution compared to a simpler Δr computation based on the rotor hex vertices.

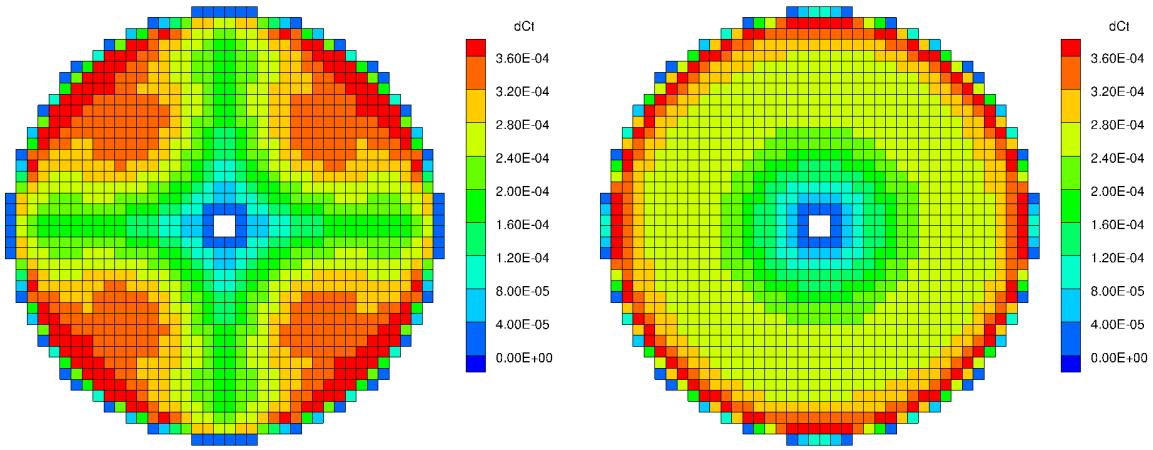

Figure 1: Comparison of definitions for Δr: simple (left) versus equivalent area (right)

For the unsteady model based on swept area, the same principle is applied using the ratio of angles. Let $\Delta\Phi = \Omega\Delta t$ be the swept area (wedge) angle and $\Delta\psi$ remain as defined above for the steady model. Now the scaling factor is

$$f_{sc} = g\left(\Delta\Phi\right)\Delta\psi = g\left(\Delta\Phi\right)\frac{A_c}{r\Delta r} \tag{6}$$

where $g\left(\Delta\Phi\right)$ is probability density function of a statistical distribution. This ensures that the blade element forces are scaled such that if $\Delta\Phi = N_b/(2\pi)$ and a boxcar distribution is chosen, the unsteady model reverts to the steady formulation. However, in order to maintain a smooth force distribution throughout the rotor plane, the unsteady forces are smoothed using a generalized trapezoidal function instead of the discontinuous boxcar function. The resulting force scaling is similar to [4] except for the choice of statistical distribtuion.

3.3 Airfoil Tables and Interpolation

Table lookups are used to determine airfoil lift and drag coefficients in the blade element model based on local flow conditions. We use multi-linear interpolation over angle of attack and Mach number between tables specified at each radial station. The interpolation is implemented in a hypercube approach utilizing regularized tables with fixed angles of attack (124 pts) and Mach numbers (28 pts). The basic framework for Reynolds number interpolation between airfoil tables has been developed but the presented results do not utilize this feature.

3.4 Parallelization and Load Balancing

The Cartesian flow solver is parallelized with either OpenMP and MPI, which decompose the computational domain via space filling curves into subdomains spread across the processors [1]. The current model is implemented in the OpenMP solver, but the extension to a distributed memory framework is expected to be fairly straightforward.

Load balancing is accomplished by distributing the rotor hexes across all compute cores which parallelizes the rotor model body force computation over all available threads. *The final paper will include some simple parallel scaling results.*

4 Computational Results

In this work, we first investigate the mesh convergence of the rotor model and then proceed onto comparisons of XV-15 hover performance predictions with both experimental data [3] and numerical simulations [11]. The applicability of the model to multi-rotor aircraft is then investigated by comparison to recent work by Yoon, Lee, and Pulliam [14], in which they considered the effect of rotor separation distance on total thrust for a notional quadrotor vehicle.

4.1 Mesh Convergence

Since the proposed rotor model uses the existing computational mesh instead of an embedded polar mesh, it is prudent to show that the model converges as the grid is refined. We use a simplified rotor with linear twist, rectangular planform, constant thickness, and uniform cross section (airfoil) along the span. Even so, for a steady rotor hovering in an inviscid fluid, this is a non-trivial task as mesh refinement reduces dissipation in the wake shear layer which may then go unsteady. Nonetheless, we are able to show reasonable mesh convergence of thrust and torque with about 10000 cells, as shown in figure 2. *The final paper will also include mesh convergence results for the unsteady rotor model.*

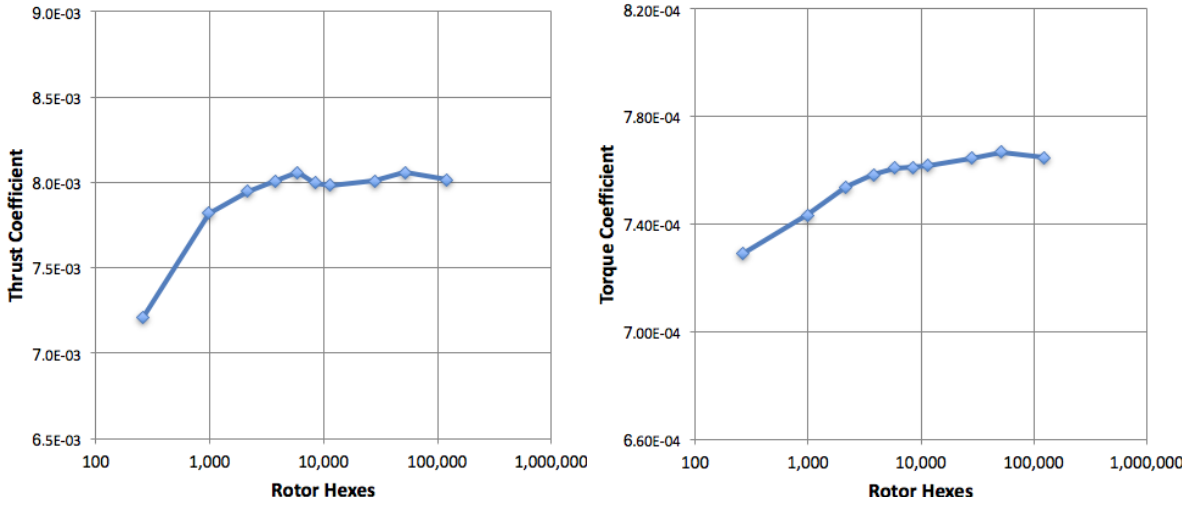

Figure 2: Mesh convergence of rotor model: thrust (left) and torque (right)

4.2 XV-15 Rotor

Since the model treats the rotor as a thin disk and assumes a 2-dimensional strip (blade element) theory, it would be naive to expect the model to precisely match experimental data or high-fidelity simulations with actual rotor blade geometry. However, it is worth investigating rotor performance estimates to establish the model's suitability for aerodynamic design.

As an initial test, an isolated XV-rotor with fictitious centerbody is simulated in hover at a tip Mach number of 0.69. The rotor is assumed to be rigid and blade pre-coning is ignored. Farfield boundaries were placed 30 rotor diameters away. In figure 3 we see that the figure of merit is well predicted although the steady model stalls at a lower thrust coefficient (C_T) than in the experiment [3].

Next, we repeat the quadrotor separation distance investigation from [14] with the present rotor model. Figure 4 shows the variation of normalized thrust at several distances holding collective pitch constant (10°). Overall, the trend is well predicted, although the steady model underpredicts the isolated rotor's thrust by about 0.5% at $S/D = 2.0$. *The final paper will also include results from the unsteady rotor model and comparisons between steady, unsteady, and high-fidelity approaches.*

5 Conclusions

In this abstract, we detail the development of a rotor model which has been implemented in an adaptive Cartesian mesh framework directed at flow simulations over complex geometries. The body force implementation chosen allows for arbitrarily oriented rotors, and when coupled with Cart3D's automated meshing capabilities and solver efficiency, provides a rapid and powerful simulation capability for multi-rotor aircraft design. The model transitions seamlessly between steady and unsteady modes, using a generalized trapezoidal distribution over the cells inside the blade swept area. Parallelization is done in a shared memory context and rotor hexes are distributed among all nodes for load balancing. Good mesh convergence of thrust and torque is achieved with approximately 10000 cells for a hovering rotor, and numerical simulations of the XV-15 rotor show good correlation to both previous experimental data and high-fidelity numerical predictions for single and quadrotor configurations in hover.

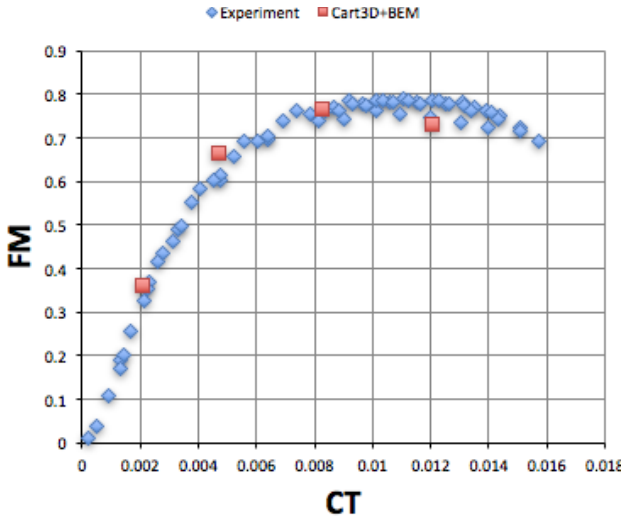

Figure 3: Figure of merit vs thrust coefficient of XV-15 Rotor

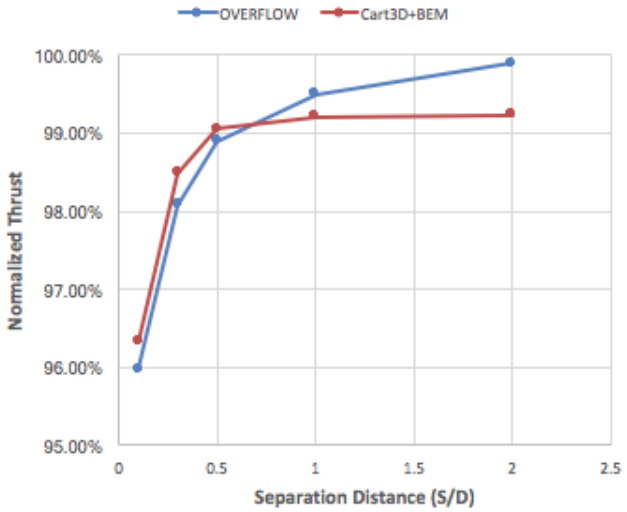

Figure 4: Normalized thrust vs separation distance of XV-15 Rotor

Acknowledgments

This work was supported by the NASA Ames Research Center contract NNA10DF26C. The authors gratefully acknowledge the assistance of Jasim Ahmad and Tom Pulliam from NASA Ames.

References

[1] Aftosmis, M. J., Berger, M. J., and Adomavicius, G. A parallel multilevel method for adaptively refined Cartesian grids with embedded boundaries. 38th Aerospace Sciences Meeting. AIAA 2000-0808.

[2] Chaderjian, N. M., and Buning, P. G. High resolution Navier-Stokes simulation of rotor wakes. AHS International 67th Annual Forum.

[3] Felker, F. F., Betzina, M. D., and Signor, D. B. Performance and loads data from a hover test of a full-scale XV-15 rotor. NASA-TM-86833.

[4] Forsythe, J. R., Lynch, E., Polsky, S., and Spalart, P. Coupled flight simulator and CFD calculations of ship airwake using Kestrel. 53rd Aerospace Sciences Meeting. AIAA 2015-0556.

[5] Hariharan, N. S., Egolf, T. A., Narducci, R., and Sankar, L. N. Helicopter rotor aerodynamic modeling in hover: AIAA standardized hover evaluations. 53rd Aerospace Sciences Meeting. AIAA 2015-1242.

[6] Jameson, A. Time dependent calculations using multigrid, with applications to unsteady flows past airfoils and wings. 10th Computational Fluid Dynamics Conference. AIAA 1991-1596.

[7] Le Chuiton, F. Actuator disc modelling for helicopter rotors. *Aerospace Science and Technology 8*, 4 (2004), 285–297.

[8] Leishman, G. J. *Principles of helicopter aerodynamics*. Cambridge university press, 2006, pp. 115–119.

[9] O'Brien Jr, D. M. *Analysis of computational modeling techniques for complete rotorcraft configurations*. PhD thesis, Georgia Institute of Technology, 2006.

[10] Shen, W. Z., Sørensen, J. N., and Zhang, J. Actuator surface model for wind turbine flow computations. 2007 European Wind Energy Conference and Exhibition.

[11] Sheng, C., Zhao, Q., and Hill, M. Investigations of XV-15 rotor hover performance and flow field using U2NCLE and Helios codes. 54th AIAA Aerospace Sciences Meeting. AIAA 2016-0303.

[12] Tadghighi, H. Simulation of rotor-body interactional aerodynamics- an unsteady rotor source distributed disk model. AHS International 57th Annual Forum.

[13] Wissink, A., Jayaraman, B., Datta, A., Sitaraman, J., Potsdam, M., Kamkar, S., Mavriplis, D., Yang, Z., Jain, R., Lim, J., and Strawn, R. Capability enhancements in Version 3 of the Helios high-fidelity rotorcraft simulation code. 50th Aerospace Sciences Meeting. AIAA 2012-0713.

[14] Yoon, S., Lee, H. C., and Pulliam, T. H. Computational analysis of multi-rotor flows. 54th Aerospace Sciences Meeting. AIAA 2016-0812.